

Low-order moment expansions to tight binding for interatomic potentials: Successes and failures

Joel D. Kress and Arthur F. Voter

Theoretical Division (T-12, MS B268), Los Alamos National Laboratory, Los Alamos, New Mexico 87545

(Received 23 January 1995)

We discuss the use of moment-based approximations to tight binding. Using a maximum entropy form for the electronic density of states, we show that a general interatomic potential can be defined that is suitable for molecular-dynamics simulations and has several other desirable features. For covalent materials (C and Si), properties where the atoms are in equivalent environments are well converged at low-order moments. For defect environments, which offer a more critical (and relevant) test, the method is found to give less satisfactory results. For example, the vacancy formation energy for Si is too low by ~ 2 eV at 10 moments relative to exact tight binding. Attempts to improve the accuracy were unsuccessful, leading to the conclusion that potentials based on this approach are inadequate for covalent materials. We speculate that this may be a deficiency of low-order moment methods in general. For metals, in contrast to the covalent systems, we find that the low-order moment approach is better behaved. This finding is consistent with the success of existing empirical fourth-moment potentials for metals.

I. INTRODUCTION

Atomistic simulations are playing an increasing role in the design and understanding of modern materials. Because the predicted properties are only as accurate as the interatomic potentials used in the simulation, the development of improved potentials is currently receiving much attention. The "ideal" potential would be closely based on electronic structure principles; it would be applicable to a wide range of bonding types (i.e., metallic, covalent, ionic); it would describe a range of densities (solids, liquids), symmetries (crystals, surfaces, clusters), and coordination number; it would allow for bond dissociation; it would be easily parametrized for new systems; and it would be computationally efficient. The last requirement is diametrically opposed to the others and must be balanced accordingly. Many empirical potentials exist that work for limited classes of materials. For example, effective-medium-based methods¹⁻⁴ work well for metals. For covalent systems, a different approach is required, because angular terms are required to model the strong directional bonding. Specialized potentials with explicit three-body terms have been developed for the group-IV elements and hydrocarbons. Empirical potentials that describe metallic-covalent alloys are virtually nonexistent.

The tight-binding total-energy method (TB) may fill this gap. TB parameters exist for both metals and covalent materials and the description of alloys appears straightforward. Traditional TB methods require the diagonalization of the tight-binding Hamiltonian matrix, for which the computational work scales as N^3 (N is the order of the TB matrix). This severely limits the number of atoms that can be simulated in a practical sense, and has spurred the development of approximations that scale as N . These N -scaling methods generally fall into two categories: those based on the moments of the electronic density of states (DOS), and the more recently proposed

iterative solutions for generating the density matrix^{5,6} or eigenvectors⁷⁻¹⁰ directly. The moment-based approach is the subject of the present paper.

In this paper we report on attempts to develop a general moment approach that is suitable for molecular-dynamics simulations. We construct low-order moments $(0, 1, 2, \dots, n_{\max})$ of a tight-binding Hamiltonian. The DOS is characterized with a maximum entropy (ME) solution that satisfies the $n_{\max} + 1$ moment constraints. The DOS is filled with valence electrons and an electronic energy is computed. This method has many attractive features: (1) ME makes the best possible use of limited moment information in a statistical sense; (2) large n_{\max} converges to the exact-TB (diagonalized) limit; (3) n_{\max} can be chosen to trade accuracy for speed; (4) the valence electron filling is based on chemical identity; (5) semi-quantitative electronic structure information is obtained because a DOS is constructed; (6) one can use existing TB parameter sets, avoiding parametrization studies; and (7) the method is suitable for molecular dynamics.

For metallic systems, successful potential forms have been developed that correspond to a simple second-moment approximation.^{4,11} Some potentials based on methods beyond the second moment have been published.¹²⁻¹⁷ Interatomic potentials for Si (Ref. 14) and for half-filled d -band metals¹⁵ (Cr, Mo, and W) using up to and including fourth moments have been presented. The electronic energy is based on the eigenvalues of the second-moment matrix and a linear function of the fourth moment scaled by the $\frac{3}{2}$ -root of the second moment. In this manner the question of the density of states is bypassed. In addition, for the Si potential, a dipole term was added.

Pettifor¹² has proposed a many-body potential based on the moments of the bond order (a bond orbital versus an atomic orbital basis). Instead of constructing the DOS that exactly reproduces the first n_{\max} moments, a perturbation theory treatment is used that generates an average

DOS that captures the essence of the many-body behavior of the true DOS. For example, Pettifor and Aoki¹⁸ have applied this approach up through sixth moment in an analysis of the hcp/bcc/fcc stability of transition metals, and Alinaghian *et al.*¹⁹ have examined *s*- and *sp*-valent systems with a fourth-moment approximation.

The recursion method^{20–22} can also be viewed as a moment-based method. In a study relevant to the goals of the present paper, Glanville, Paxton, and Finnis²³ compared the recursion method with the ME method as applied to *d*-band metal calculations of the tight-binding electronic energy for fcc, hcp, and bcc structures. Other relevant recursion studies of Si include those of Paxton, Sutton, and Nex²⁴ and Paxton.²⁵

Brown and Carlsson²⁶ investigated low-order moment expansions for the calculation of the electronic energy of lattices and defects of *d*-band materials. They considered various schemes for truncating approximations to the DOS and concluded that the best results were obtained with the ME and recursion methods. Recently, Drabold and Sankey²⁷ have proposed an *N*-scaling statistical approach that uses the ME principle and random vectors to generate highly accurate estimates for moments. They have applied this to a tight-binding description of optical phonons in GaAs and the structure of large fullerenes (up to 2160 atoms).

In this paper, we address the question of whether a useful approximation to TB can be found for a few moments, and discuss the suitability of moment-based methods in general for describing covalent and metallic materials. We are led to the unfortunate conclusion that low-order moment methods (i.e., $n_{\max} \lesssim 10$) probably are not suitable for an accurate description of covalent materials. Examination of the simplest possible point defect, an unrelaxed vacancy, is sufficient to demonstrate the inadequacies of the moment approach. However, a study restricted to properties of nondefective solids [e.g., lattice constant, cohesive energy, elastic constants, structural energy differences] can lead to the incorrect conclusion that the method works well, converging quickly to the exact-TB limit. For metals, the convergence properties of a low-order moment expansion appear to be better behaved.

II. THEORY

A. Moments and density of states

We begin by expressing the total energy of the system as

$$E_{\text{tot}} = E_{\text{elec}} + E_{\text{pair}}. \quad (1)$$

E_{elec} is the electronic energy and

$$E_{\text{pair}} = \frac{1}{2} \sum_i \sum_{j(\neq i)} \phi(r_{ij}), \quad (2)$$

where $\phi(r_{ij})$ is a pairwise potential, a function of the internuclear distance $r_{ij} = |\mathbf{r}_{ij}|$, representing core-core interactions and neglected contributions to the true electronic energy, such as double-counting terms. (Throughout, sums over Roman indices are sums over

atoms.) The electronic energy is defined as²⁸

$$E_{\text{elec}} = 2 \int_{-\infty}^{E_F} \epsilon n(\epsilon) d\epsilon, \quad (3)$$

where $n(\epsilon)$ is the total electronic density of states and the factor of two accounts for the closed-shell spin state (two electrons per orbital). The form of Eq. (1) can be justified within the Harris-Foulkes^{29,30} variational scheme as an approximate solution to the density-functional ground-state energy. The Fermi energy E_F is found from

$$N_{\text{val}} = 2 \int_{-\infty}^{E_F} n(\epsilon) d\epsilon, \quad (4)$$

where $N_{\text{val}} = \sum_i N_{\text{val},i} n_{\text{atom}}$ is the number of atoms in the system, and $N_{\text{val},i}$ is the number of valence electrons on atom *i*. The total DOS can be expressed as

$$n(\epsilon) = \sum_i n_i(\epsilon), \quad (5)$$

where $n_i(\epsilon)$ is the DOS projected onto atom *i*. If desired, a local Fermi energy, $E_{F,i}$, can be determined for each atom DOS (instead of determining a single global E_F), via

$$N_{\text{val},i} = 2 \int_{-\infty}^{E_{F,i}} n_i(\epsilon) d\epsilon. \quad (6)$$

For a single component system with all atoms equivalent, $E_{F,i} = E_F$ for all atoms *i*.

The electronic energy is based on a one-electron TB model for the system. The exact total DOS, $n(\epsilon)$, can be determined by diagonalizing the TB Hamiltonian, although this is only practical for systems containing less than $\sim 10^3$ atoms. Instead, we characterize the DOS from its energy moments. The *m*th moment projected onto atom *i* is

$$\mu_{mi} = \int_{-\infty}^{\infty} \epsilon^m n_i(\epsilon) d\epsilon. \quad (7)$$

The moments can be computed³¹ for orbital $|i, \alpha\rangle$ as

$$\mu_{mi\alpha} = \langle i, \alpha | \hat{H}^m | i, \alpha \rangle, \quad (8)$$

where $\alpha = 1, \dots, n_{\text{orb}}$ is the angular momentum index ($s, p_x, \dots, d_{xy}, \dots$) and \hat{H} is the TB Hamiltonian. The energy of $|i, \alpha\rangle$ for an isolated atom is $\epsilon_{i,\alpha}^0$. A trace over orbitals yields the atom moment,

$$\mu_{mi} = \sum_{\alpha} \mu_{mi\alpha} \quad (9)$$

which is invariant with respect to rotations of the coordinate system. The global *m*th moment is given by

$$\mu_m = \sum_i \mu_{mi} = \text{Tr}[\hat{H}^m]. \quad (10)$$

The zeroth and first moments are evaluated trivially as $\mu_{0i\alpha} = \langle i, \alpha | i, \alpha \rangle = 1$, and $\mu_{1i\alpha} = \langle i, \alpha | \hat{H} | i, \alpha \rangle = \epsilon_{i,\alpha}^0$, respectively. For moments higher than first, Eq. (8) is evaluated by inserting a complete set of orbitals. For example,

$$\begin{aligned} \mu_{2i\alpha} &= \sum_j \sum_{\beta} \langle i, \alpha | \hat{H} | j, \beta \rangle \langle j, \beta | \hat{H} | i, \alpha \rangle \\ &= [H_{i\alpha, j\beta}]^2. \end{aligned} \quad (11)$$

The TB matrix elements $\langle i, \alpha | \hat{H} | j, \beta \rangle = h_{\alpha\beta}(\mathbf{r}_{ij})$ in Eq.

(11) are assumed to have a two-center form; the radial dependencies are parametrized and the angular dependencies are determined by the Slater-Koster relations.³² Note that the sum over i in Eq. (11) includes $i=j$ terms, which give rise to self-energy factors such as $\epsilon_{i,\alpha}^0$.

Improved TB models exist in which many-body effects are incorporated by defining the two-center matrix elements that depend on the local environment of the two atoms.³³ That type of scheme is compatible with the approach presented here. It would increase the time spent defining the two-center matrix elements without affecting the work to evaluate the moments and DOS.

Rotational invariance of the moments, and hence the energy expression, is crucial in designing a useful potential. The common approach of tracing the moments over the orbitals of each atom [Eq. (9)] offers rotational invariance while providing more information about the system than the global moments. Although the individual orbital moments are *not* rotationally invariant, there are ways to define invariant submoments of a given atom. One approach^{14,34} is to use the eigenvalues of the m th-moment matrix

$$[\mu_{mi}]_{\alpha,\beta} = \sum_j \sum_{\beta'} \langle i, \alpha | \hat{H}^m | i, \beta' \rangle. \quad (12)$$

Another approach, which we refer to as the “shell-trace” method, is to sum individual angular momentum shells independently. For Si, this leads to an s trace ($[\mu_{mi}]_{s,s}$) and a p trace ($[\mu_{mi}]_{x,x} + [\mu_{mi}]_{y,y} + [\mu_{mi}]_{z,z}$).

If an s -orbital basis is used, the second moment becomes a scalar. The second moment approximation⁴ energy expression $E_{\text{elec},i} = -\sqrt{\mu_{2i}}$ can be derived³⁵ by neglecting the first moment and using a half-filled Gaussian DOS.

B. Maximum entropy method

The best approximation (in a statistical sense) to the DOS given the first n_{max} moments ($0, 1, \dots, n_{\text{max}}$) is the maximum entropy solution.³⁶ Mead and Papanicolaou³⁷ demonstrated the usefulness of the ME approach for various applications in mathematical physics. Brown and Carlsson²⁶ applied ME to low-order moment expansions of the DOS for d -band materials.

In the ME approach, one maximizes Shannon’s entropy,

$$S = - \int_{\epsilon_{\text{bot}}}^{\epsilon_{\text{top}}} n(\epsilon) \log[n(\epsilon)] d\epsilon, \quad (13)$$

subject to the $n_{\text{max}} + 1$ moment constraints. The solution is

$$n(\epsilon) = \exp \left[\sum_j \lambda_j \epsilon^j \right], \quad j = 0, 1, \dots, n_{\text{max}}, \quad (14)$$

where the $\{\lambda_j\}$ are coefficients determined from a non-linear search for the solution with zero error in the predicted moments. This is usually accomplished using a Newton-Raphson (NR) algorithm. As expected from the derivation, the ME method gives the smoothest (least-peaked) distribution that satisfies the moment conditions. Nonetheless, it can yield quite peaked shapes if necessary.

For example, $n_{\text{max}}=2$ yields a Gaussian and $n_{\text{max}}=4$ cases are typically smooth, bimodal distributions; yet, for $n_{\text{max}}=4$ with $\mu_4 = [\mu_2]^2$ ($\mu_1 = \mu_3 = 0$), the only possible solution, two delta functions positioned at $\pm\sqrt{\mu_2}$, comes out naturally from Eq. (14).

As pointed out by Glanville, Paxton, and Finnis²³ and Turek,³⁸ the ME solution is often hard to converge. The transformation method of Bretthorst³⁹ helps in this regard. (We were able to obtain stable solutions for n_{max} up to ~ 20 .) However, once a ME solution has been converged, reconverging for similar moments requires only two or three iterations in a standard NR procedure, without any need for transformation. By exploiting this feature, the ME approach can be used effectively in molecular dynamics (MD). The new electronic energy at each time step is quickly found, as are the numerical derivatives of the electronic energy with respect to the moments, which require only one NR iteration.

Note that E_{elec} depends parametrically on the choice of ϵ_{bot} and ϵ_{top} in Eq. (13). We find that this dependence is weak if they are chosen such that the distribution decays to nearly zero at the limits.

C. Procedure

We now discuss the steps for computing the energy in this ME approach. First, the appropriate orbital basis and the form for the radial hopping integrals are chosen. For Si, this would be an sp basis, with $h(r)$ specified for $ss\sigma$, $sp\sigma$, $pp\sigma$, and $pp\pi$ interactions. For a given geometry of the atoms, the pair energy is computed from Eq. (2) and the moments $\{\mu_{mi}\alpha\}$ are computed for each orbital in the system. The m th moment of orbital α on atom i is the sum over all possible paths having m links that start and end on orbital $|i,\alpha\rangle$. Orbitals $|i,\alpha\rangle$ and $|j,\beta\rangle$ are “linked” if $H_{i\alpha,j\beta} \neq 0$, as determined by the cutoff range of $h_{\alpha\beta}(r_{ij})$, which is typically one or two neighbor shells. The contribution from each path is the product of the m matrix elements. Path links that begin and end on the same atom j are included, contributing $\delta_{\alpha\beta} \epsilon_{j\alpha}^0$ to the product. Forming partial products (e.g., all products with k links beginning on atom i and ending on atom j) speeds the evaluation. Once the moments have been computed for every orbital, a rotationally invariant set is obtained by either tracing over the whole system [“global trace,” Eq. (10)], over each atom [“atom trace,” Eq. (9)], or over each angular momentum shell on each atom (“shell trace”). For each traced set of moments, a DOS is found using the ME procedure discussed above. Given these DOS’s, we define five methods for calculating a total electronic energy for the system, as discussed next.

In the “global-trace” method, the single DOS constructed from the fully traced moments is populated with electrons to define a single, total electronic energy, using Eqs. (4) and (3). In the “atom-trace” method, the global DOS is defined as the sum over the atom DOS’s, each constructed from a separate ME solution using atom-traced moments, and this global DOS is populated with electrons to determine a single electronic energy. The “shell-trace” method is analogous to the atom-trace

method, with the global DOS summed over the DOS's for every angular momentum shell for every atom. The advantage of the atom-trace and shell-trace methods over the global-trace method is that they provide successively more detail in the DOS, while retaining the correct overall moments. All three of these approaches have a global Fermi level, allowing charge transfer among the atoms. Also, all three converge rigorously to the exact-TB energy (obtained from exact diagonalization of the TB Hamiltonian) as $n_{\max} \rightarrow \infty$.

Alternatively, the atom DOS's can be populated individually as in Eq. (6), leading to an electronic energy for each atom, so the total electronic energy is given by $E_{\text{elec}} = \sum_i E_{\text{elec},i}$. This modification can be made to either the atom-trace or the shell-trace methods, leading to our definition of the "charge-neutral atom-trace" and "charge-neutral shell-trace" methods, respectively. Although these two methods do not converge to exact TB with large n_{\max} , they are consistent with arguments made by Sutton *et al.*²⁸ that enforcing charge neutrality on each atom leads to a higher-quality TB approximation. They also offer the advantage that an energy can be defined for each atom. If desired, this same charge neutrality constraint can be applied to exact TB. This is accomplished, after diagonalization, by using the eigenvectors and eigenvalues to project out the DOS for each atom. This will be referred to as charge-neutral exact TB.

In comparing the methods, we observe that the rate of convergence to exact TB improves in going from global trace to atom trace to shell trace, as might be expected because of the extra detail in the DOS. Also, the charge-neutral-atom-trace energy is greater than or equal to the atom-trace energy (and similarly for the charge-neutral shell-trace energy relative to the shell-trace energy), because the charge transfer that occurs in going from local Fermi levels to a global Fermi level can only lower the energy.

For systems in which all atoms are equivalent, the charge-neutral methods are equivalent to their global-Fermi-level counterparts. Also, because the global-trace moment is then equal to the atom-traced moments (within a normalization factor), the atom-trace and global-trace methods are equivalent.

The shell-trace and atom-trace methods require more computation than the global-trace methods because multiple ME searches must be performed. However, for $n_{\max} \geq 4$ this extra work becomes negligible once good starting guesses for $\{\lambda_j\}$ have been found (e.g., from a previous MD step).

The boundary conditions (BC's) in the calculations presented below are either periodic or infinite. For the "infinite" BC's, a sufficiently large cluster is carved out around each atom such that the moment loops sense an infinite crystal. For infinite BC's, only the charge-neutral methods can be used, because the total number of electrons in the system is undefined. In the periodic-BC calculations, the moment loops can wrap around as n_{\max} is increased, leading to different results than the infinite BC's. The advantage of periodic BC's is that direct comparisons can be made with exact-TB calculations.

III. RESULTS

To determine the accuracy of the ME method, we compare to exact TB, which is defined as the exact diagonalization of a TB Hamiltonian for a system of a given size. This properly determines the accuracy of the approximation and decouples the issue of the accuracy of the TB Hamiltonian itself.

Electronic energies are calculated with respect to the separated atom limit. For $n_{\max} < 4$, there is an ambiguity in the calculation of the isolated atom electronic energy for *sp*-orbital systems, because the ME solution does not yield separate delta functions (atomic levels). For this reason, $n_{\max} < 4$ results are not shown.

The N -atom vacancy formation energy is defined as $\Delta E_{\text{vac}} = E^{N-1} - E^N(N-1)/N$ where E^N is the energy of an N -atom periodic system and E^{N-1} is the *unrelaxed* energy of the system with one atom removed. Similarly, the N -atom interstitial formation energy is defined as $\Delta E_{\text{int}} = E^{N+1} - E^N(N+1)/N$ where E^{N+1} is the *unrelaxed* energy of the system with one atom added. Because the defect region is not allowed to relax, the absolute error in the electronic energy contribution equals the absolute error in the total vacancy or interstitial energy. Using the relaxed defect energy would unnecessarily complicate matters, because it would contain contributions from the moment approximation we are testing as well as from the interplay between the pair potential and the TB Hamiltonian.

A. Covalent materials

For Si, the TB parameters of Goodwin, Skinner, and Pettifor⁴⁰ were utilized. Exact-TB results for up to 1000 atoms ($5 \times 5 \times 5$ supercell, $a_0 = 10.259$ bohrs, 1 bohr = 0.5292 Å) were generated. First nearest neighbors (NN's) only were used for the calculation of the cohesive energy (E_{coh}), surface energy, ΔE_{vac} , and ΔE_{int} , while the full range potential (which is only slightly different, essentially cut off between first and second NN's) was used for the calculation of the equilibrium lattice constant and bulk modulus. Exact-TB values for ΔE_{vac} and ΔE_{int} using this potential have been reported previously by Wang, Chan, and Ho⁴¹ for the 64-, 216-, and 512-atom periodic systems.

First, properties of the bulk diamond lattice are considered. Because the atoms in the perfect lattice are equivalent, the charge-neutral and global-Fermi-level calculations are identical, as are atom trace and global trace. The Si DOS for $n_{\max} = 2, 4, \text{ and } 10$ are shown in Fig. 1(a). By the tenth moment, the bandgap (near energy = 0) is readily apparent. In Fig. 1(b), the $n_{\max} = 20$ DOS and the exact-TB DOS for the 216-atom periodic system are shown. As can be seen in Fig. 2, E_{coh} converges quickly with the number of moments; this is consistent with previous recursion studies.^{24,25} The error at $n_{\max} = 10$, relative to the 216-atom exact-TB result, is 0.08 eV/atom for a periodic 216-atom system using the global-trace method. Changing to infinite BC's is seen to have almost no effect. The results change a little when the shell-trace

moments are used, offering slightly faster convergence. Figure 3 shows the equilibrium lattice constant (a_0) as a function of n_{\max} , calculated for the 216-atom periodic system. The error at $n_{\max}=6$ and 10, with respect to the exact-TB result of 10.48 bohrs, is 1% and 0.2%, respectively. The bulk modulus (B), also shown in Fig. 3, is calculated at the equilibrium a_0 for each n_{\max} . B converges more erratically than E_{coh} , perhaps not surprising for a second-derivative property. Above $n_{\max}=10$, the value of B become sensitive to the numerical details of the moment evaluation and ME determination, leading to variations of $\sim 5\%$.

Next, a planar defect is considered, the Si(100) surface. Figure 4 shows the unrelaxed surface energy (γ_{100}) calculated using a 288-atom slab ($3 \times 3 \times 4$ unit cell) with free surfaces normal to the z direction. The exact-TB result is 1778 ergs/cm². (This changes only slightly, to 1783 ergs/cm², if the slab size is increased to $4 \times 4 \times 4$ with 512 atoms.) The global-trace and atom-trace methods are

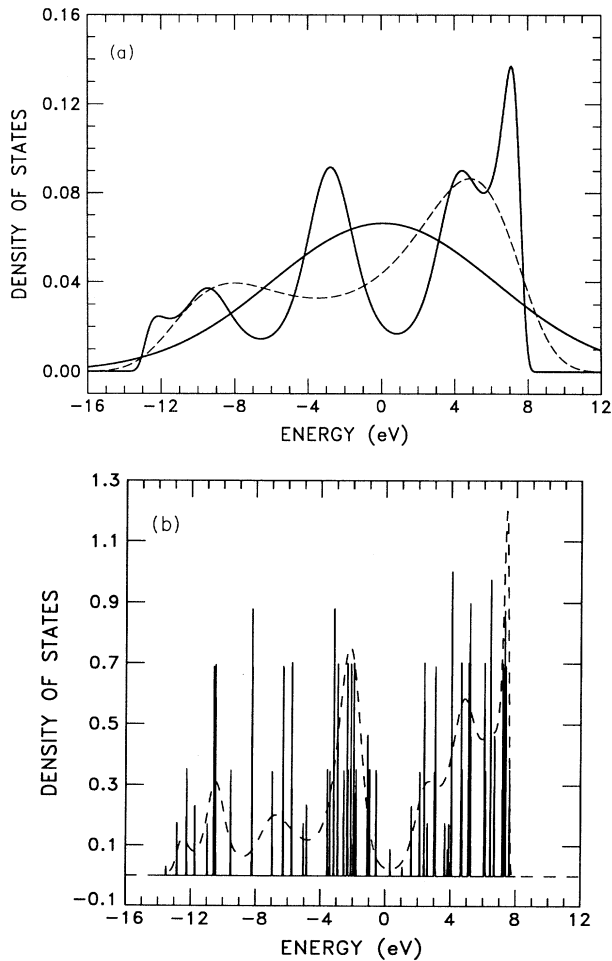


FIG. 1. (a) Si DOS (global trace). Solid line (Gaussian), $n_{\max}=2$. Dashed line, $n_{\max}=4$. Solid line (multimodal distribution), $n_{\max}=10$. (b) Si DOS. Dashed line, $n_{\max}=20$ (global trace). Solid line, exact TB for 216 periodic system convoluted with a Gaussian of negligible width. Each DOS in (b) is scaled arbitrarily for clarity. The exact-TB Fermi energy is 0.31 eV.

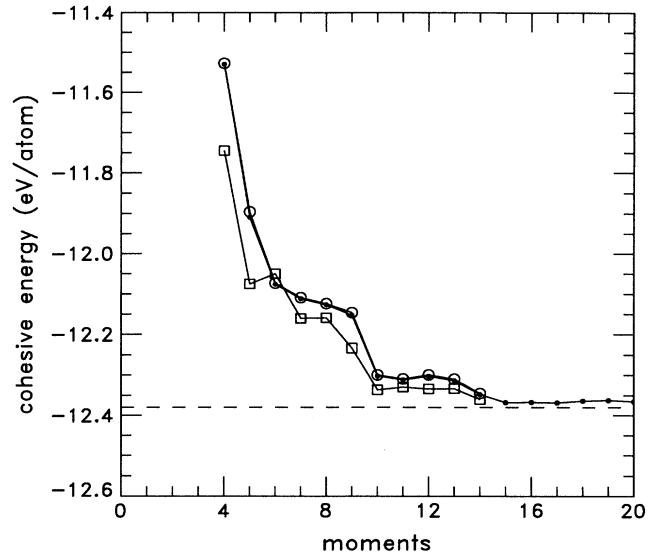


FIG. 2. Si E_{coh} vs n_{\max} (electronic energy contribution only). (●) periodic 216-atom system, global or atom trace; (○) infinite BC's, charge-neutral atom trace; (□) infinite BC's, charge-neutral shell trace. The exact-TB result for 216 atoms is indicated by the dashed line.

seen to give very similar results. The error of ~ 70 ergs/cm² at 20 moments corresponds to about 0.01 eV/atom, which is consistent with the order of magnitude of residual error in the perfect crystal energy in Fig. 2. Because the atoms in this system are not equivalent, charge transfer occurs. Imposing charge neutrality thus raises the predicted surface energy because the perfect-crystal reference system is unaffected by this constraint. This is a general feature of the methods: the charge-neutral methods always predict a higher defect energy than their global-Fermi-level counterparts. The charge-

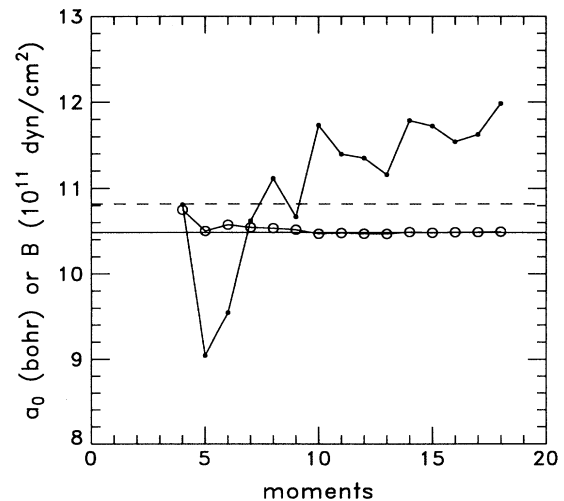


FIG. 3. Si equilibrium lattice constant (a_0 , in bohr) and bulk modulus (B , in 10^{11} dyn/cm²) vs n_{\max} for a periodic 216-atom system using the global trace method. (○) a_0 ; (●) B . The exact-TB result is the solid line for a_0 and dashed line for B .

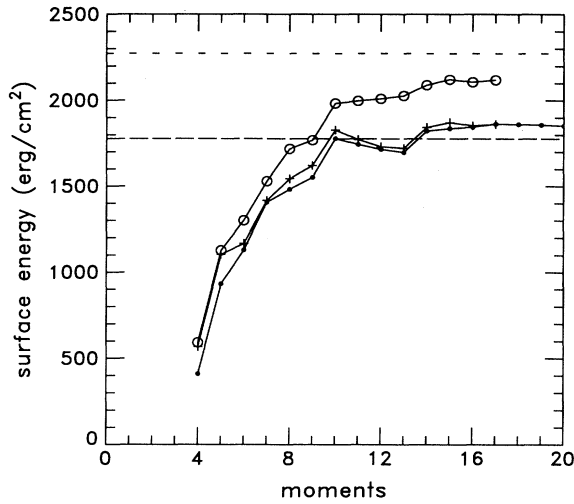


FIG. 4. Unrelaxed Si(100) surface energy for a periodic system with 288 atoms. (●) global trace; (+) atom trace; (○) charge-neutral atom trace. The exact-TB result is indicated by the long-dashed line and the charge-neutral exact-TB result is indicated by the short-dashed line.

neutral-atom-trace prediction of γ_{100} is seen to be converging towards the 2272-erg/cm² value obtained using charge-neutral exact TB.

Finally, two point defects are considered, a vacancy and an interstitial. Figure 5(a) shows the unrelaxed vacancy formation energy for a 216-atom periodic system. As indicated, the exact-TB result is 5.8 eV. Although the convergence is smooth, at 19 moments the error is still -1.6 eV for the global-trace method, and -1.4 eV for the atom-trace method. The magnitude of these errors is somewhat surprising, given the accuracy shown in Fig. 2 for the perfect crystal energy. Restricting charge transfer has little effect on the system; the charge-neutral atom-trace method raises ΔE_{vac} by 0.1 eV relative to the atom-trace method. Imposing charge neutrality on the exact-TB solution changes the 5.8-eV value by less than 0.01 eV, which is not discernible in Fig. 5(a).

The disagreement between the moment predictions and exact TB is even greater for a vacancy in an infinite system, as shown in Fig. 5(b). (The rotated-orbital results are discussed in Sec. IV.) Although exact-TB computation for an infinitely large cluster is not feasible, examination of ΔE_{vac} for a succession of clusters indicates that it increases with cluster size and is close to convergence at 1000 atoms [$\Delta E_{\text{vac}}(64)=5.0$ eV, $\Delta E_{\text{vac}}(216)=5.8$ eV, $\Delta E_{\text{vac}}(512)=6.0$ eV, $\Delta E_{\text{vac}}(1000)=6.1$ eV]. The 1000-atom value of 6.1 eV is shown as an approximation to the infinite limit in Fig. 5(b), while the true value probably lies slightly higher. Here the remaining error at 14 moments is about 2 eV.

The unrelaxed tetrahedral interstitial formation energy [ΔE_{int}] for a periodic 216-atom system is shown in Fig. 6, where only the E_{elec} contribution is plotted ($E_{\text{pair}}=14.23$ eV). Unlike the vacancy energy, the convergence is oscillatory, and the atom-trace calculations show qualitatively better behavior (much smaller oscilla-

tions) than the global-trace results. The accuracy at 15 moments is comparable to or slightly better than that for the vacancy.

As a second example of a covalent system, we have applied the ME method to carbon using the first-NN TB parameters of Wang, Chan, and Ho.⁴¹ Focusing on a 512-atom periodic system ($4 \times 4 \times 4$ supercell, $a_0=6.7245$ bohrs), the cohesive energy converges in a fashion similar to Si, with an error of $+0.005$ eV by $n_{\text{max}}=10$. (The exact TB $E_{\text{elec}}=-44.453$ eV.) Figure 7 shows the E_{elec} contribution (no pair potential) to the vacancy formation energy. As for Si, the convergence is from below, with a remaining error at $n_{\text{max}}=20$ of -3.5 eV and -2 eV for the global-trace and charge-neutral atom-trace methods,

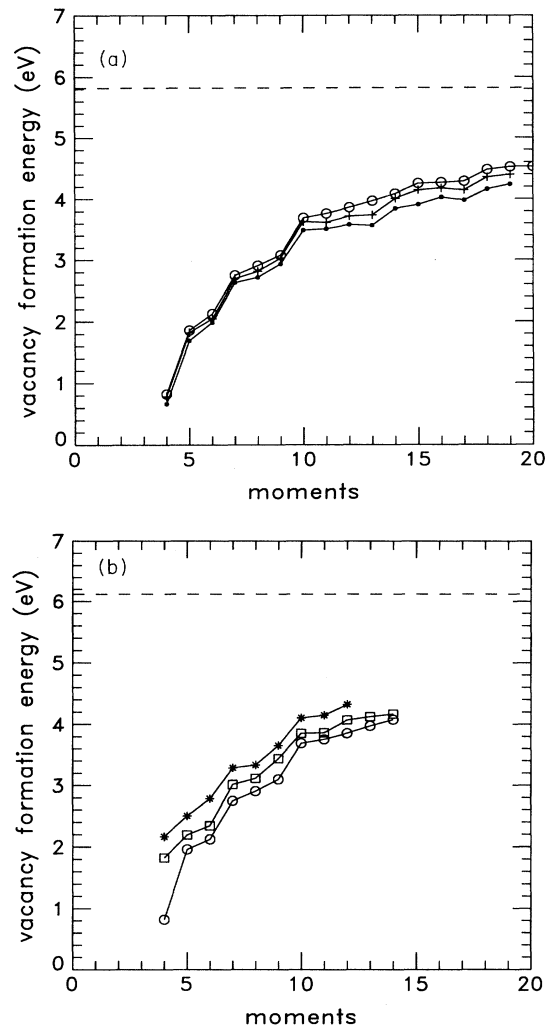


FIG. 5. Unrelaxed Si vacancy formation energy. (a) 216-atom periodic system. (●) global trace; (+) atom trace; (○) charge-neutral atom trace. The dashed line is the exact-TB result. (b) infinite BC's; (○) charge-neutral atom trace; (□) charge-neutral shell trace; (*) charge-neutral, DOS for each orbital, orbitals rotated by second-moment eigenvectors. The dashed line is the exact-TB result for a 1000-atom periodic system, which closely approximates the infinite system.

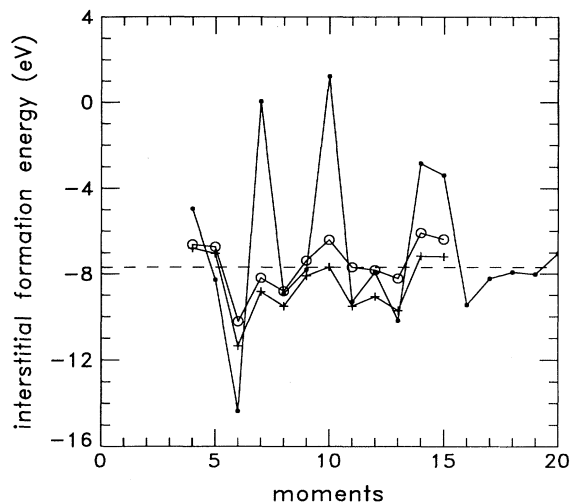


FIG. 6. Unrelaxed Si tetrahedral interstitial formation energy (electronic energy contribution only) vs n_{\max} for a 216-atom periodic system. (●) global trace; (+) atom trace; (○) charge-neutral atom trace. The exact-TB result is indicated by the dashed line.

respectively. In contrast to Si, both the global-trace and atom-trace predictions show oscillations with n_{\max} . These oscillations disappear when charge neutrality is imposed (see the charge-neutral atom-trace curve), and hence may be due to a charge-sloshing effect. Also included on Fig. 7 are the charge-neutral shell-trace results for infinite boundary conditions, which are seen to closely track the charge-neutral atom-trace values with periodic BC's.

The errors found in the point defect energies for silicon and carbon represent a serious problem for the development of an accurate interatomic potential. For Si, the

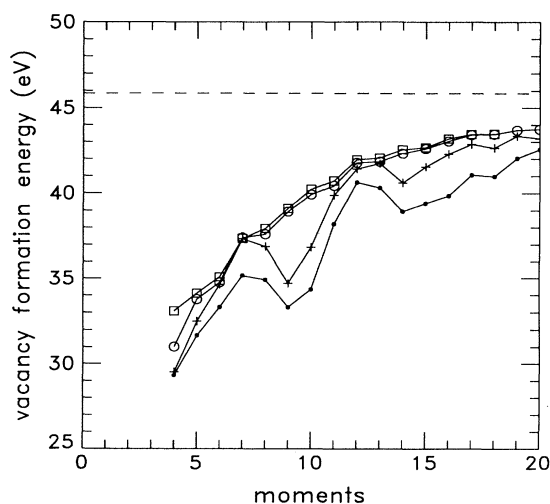


FIG. 7. Unrelaxed C vacancy formation energy (electronic energy contribution only) for a 216-atom periodic system. (●) global trace; (+) atom trace; (○) charge-neutral atom trace; (□) infinite BC's, charge-neutral shell trace. The dashed line is the exact-TB result.

predicted ΔE_{vac} is too low by 2 eV at 14 moments. At the lower values of n_{\max} (e.g., 4–8) desirable for a fast semiempirical potential, the predictions are low by 3–5 eV, and carbon is even worse. For a system at $T=1000$ K, changing ΔE_{vac} by -3 eV increases the equilibrium concentration of vacancies by 15 orders of magnitude. As discussed in the next section, we examined a number of modifications to the method in search of an improved description of the vacancy, with no success.

While we do not fully understand the reason for the poor convergence, a likely explanation is that the ME moment expansion of the DOS provides a better description of an atom adjacent to a vacancy than an atom in the bulk because the vacancy-adjacent atom has states in the band gap. Smearing of the DOS into the gap [evident even at $n_{\max}=20$; see Fig. 1(b)] raises the predicted electronic energy of the bulk system, lowering ΔE_{vac} .

Another possible explanation is that the range of the electronic perturbation about the vacancy defect reaches further than the low-order moment loops. We can rule this out in three ways. First, the extremely small change in ΔE_{vac} when comparing exact TB with charge-neutral exact TB supports the concept that the perturbation is short ranged; charge oscillations can be truncated to zero range without impacting the electronic energy significantly. Also, test calculations using a recently developed method that enhances the stability of the ME method at higher moments⁴² show that to achieve 0.5-eV accuracy requires 50 moments; the range of a 50-moment path is twice the size of the 216-atom supercell. An accuracy of 0.1 eV requires 100 moments. Finally, exact calculations within a truncated Hamiltonian space, presented elsewhere,⁴³ achieve convergence to better than 0.5 eV within a range corresponding to 10 moments. In fact, one conclusion that can be made in comparing that study with the present one is that using high-order moments ($n_{\max} \gtrsim 50$) within a short truncation range is more effective than using low- to medium-order moments, even though they reach farther.

Whatever the cause, errors of this magnitude in the Si vacancy energy at low-order moments appear to be a common feature of moment-based methods.^{44,45,46}

B. Metals

First, we consider the Skinner-Pettifor⁴⁷ s -band model for hydrogen, using a bcc lattice of 1024 atoms at $a_0=3.7$ bohrs with first- and second-NN interactions. In the exact-TB calculation, the E_{elec} contribution to E_{coh} is -38.90 eV/atom. The global-trace ME prediction of E_{coh} oscillates, with an error of $+0.8$ eV/atom at 4 moments and -0.14 eV/atom at 20 moments. Figure 8 shows the convergence of ΔE_{vac} with n_{\max} ; while the convergence is slow, the overall error (~ 0.3 eV) is much better than for the covalent systems.

Next, we considered d -band metals, for which the relevant radial hopping integrals are $dd\sigma$, $dd\pi$, and $dd\delta$.⁴⁸ Within a canonical d -band model,⁴⁹ $ddm = C_m \beta (r_{\text{NN}}/r_{ij})^5$, where $C_\sigma = -6$, $C_\pi = 4$, $C_\delta = 4$, r_{ij} is the interatomic distance, and r_{NN} is the nearest-neighbor distance. $\beta = \frac{2}{5} W (S/r_{\text{NN}})^5$, where W is the d -

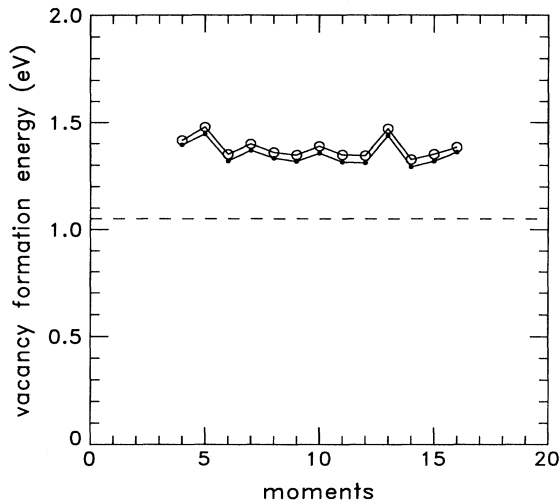


FIG. 8. Unrelaxed vacancy formation energy for bcc hydrogen. All results use a periodic 1024-atom system. (○) charge-neutral-atom trace; (●) global trace. The exact-TB result is indicated by the dashed line.

band width and S is the Wigner-Seitz radius. To maintain generality, energies are presented in units of β , and the pair potential contribution (which would be metal specific) is zero. Typical values for β are 0.16 eV for Cr, 0.24 eV for Mo, and 0.26 eV for W . Quoted rms errors refer to the average over the d -band fillings from d^1 to d^9 .

For fcc d metals, a periodic 500-atom system ($5 \times 5 \times 5$ supercell; first-NN model) was employed. The global-trace ME prediction of E_{coh} (not shown) is very good for all d -band fillings; the rms error for d^1 through d^9 is 0.45β and 0.16β for $n_{\text{max}}=4$ and 10, respectively. ΔE_{vac} is shown in Fig. 9; the rms error is 1.7β and 1.4β for $n_{\text{max}}=6$ and 20, respectively.

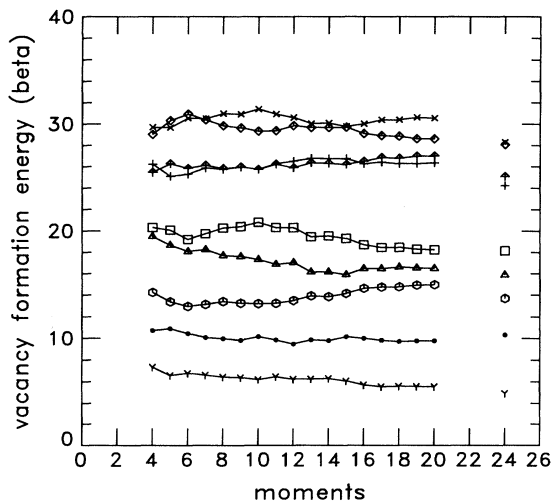


FIG. 9. Unrelaxed vacancy formation energy for fcc d metal, using the global-trace method on a periodic 500-atom system (electronic energy contribution only). (●) d^1 ; (△) d^2 ; (+) d^3 ; (×) d^4 ; (◇) d^5 ; (↑) d^6 ; (□) d^7 ; (○) d^8 ; (∇) d^9 . The exact-TB results are indicated by the $n_{\text{max}}=24$ values.

For bcc d metals, a periodic 686-atom system ($7 \times 7 \times 7$ supercell; first- and second-NN model) was employed. Again, the global-trace ME prediction of E_{coh} (not shown) is very good, with a rms error of 0.79β and 0.11β for $n_{\text{max}}=4$ and 10, respectively. ΔE_{vac} is shown in Fig. 10; the rms error is 2.4β and 1.0β for $n_{\text{max}}=6$ and 20, respectively.

To summarize, we find fast convergence with the number of moments for the cohesive energy of a variety of s - and d -band metals. This is consistent with previous ME calculations^{26,23} and recursion calculations²³ on metal systems. Furthermore, in contrast to the covalent systems, the convergence of the vacancy formation energy in metals appears adequate at low-order moments, perhaps because there is no band gap. This is consistent with the success of the empirical fourth-moment potentials for transition metals.^{15–17,50}

IV. VARIATIONS ON THE APPROACH

Because of the poor prediction of the vacancy formation energy in Si and C, the moment-based approximation to TB described above appears to be unsuitable for use as an interatomic potential in covalent materials. Using the Si vacancy formation energy as the benchmark, we examined a number of variations on this approach with the goal of finding a better approximation. All the approaches we considered were designed to converge to exact TB (or charge-neutral exact TB) in the limit of large n_{max} . None offered substantial improvement in the vacancy formation energy. For completeness, we briefly discuss these here.

Increased information about the local environment of an atom can be obtained if the moments, and a DOS, are computed for each orbital, rather than tracing over the whole shell or atom. As discussed above, the key is to

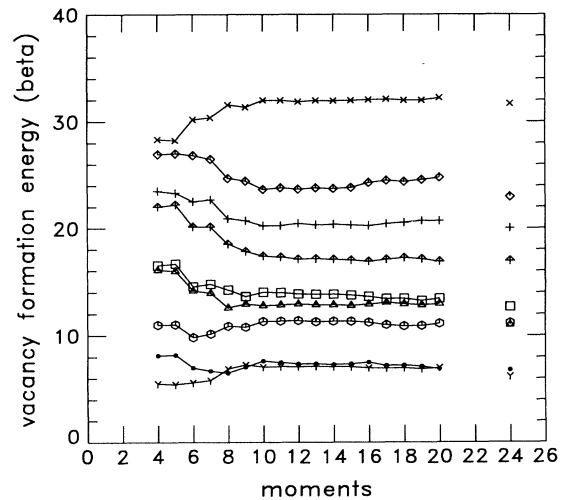


FIG. 10. Unrelaxed vacancy formation energy for bcc d -metal (electronic energy contribution only). All results use the global-trace method on a periodic 686-atom system. Same legend as Fig. 9. The exact-TB results are indicated by the $n_{\text{max}}=24$ values.

choose a definition for each orbital such that rotational invariance is maintained. One method is to diagonalize the second-moment matrix on each atom [see Eq. (12)], using the eigenvectors as the invariant set of orbitals.^{14,34} The second moment for each of these orbitals is simply the corresponding eigenvalue, while the n th moment is obtained by transforming the n th-moment matrix with the second-moment eigenvectors. (Alternatively, the eigenvectors of one of the higher-moment matrices can be used as the rotationally invariant orbital basis.) This type of approach has the disadvantage that the energy derivatives necessary for MD are not easily determined analytically, because derivatives of the eigenvector coefficients must be found. However, it offers a test of how much of the slow convergence to exact TB is due to the information lost when the moments are traced. Figure 5(b) shows that the predicted vacancy formation energy improves by about 0.2 to 0.3 eV relative to the shell-trace method (charge neutral in each case), and the improvement is fairly constant over the examined range of $n_{\max}=4-12$.

To explore the possibility that there exists *some* orbital transformation that offers even greater enhancement, we tried the following experiment. Using a random number generator, 1000 independent, 4×4 orthogonal transformation matrices were generated. One at a time, these were applied to transform the orbitals on both a bulk Si atom and a Si atom adjacent to a vacancy. Four times the energy difference between these two atoms represents a first-NN approximation to the vacancy formation energy, $\Delta E_{\text{vac}}^{(1)}$. Using $n_{\max}=4$, $\Delta E_{\text{vac}}^{(1)}$ ranged from 0.8 to 2.3 eV with an average of 1.4 eV, compared to $\Delta E_{\text{vac}}^{(1)}=2.4$ eV obtained when the second-moment eigenvectors defined the transformation. We conclude that it is very unlikely any orbital transformation exists that dramatically improves the vacancy formation energy. An interesting observation from this study was that for the atom in the perfect bulk environment, transforming using the second-moment eigenvectors gave a lower bound on the energies obtained from the random transformations. Any orbital transformation that mixed the s and p orbitals raised the energy, while rotating the p orbitals among themselves had no effect on the energy. In contrast, for the atom adjacent to the vacancy, the random transformations usually lowered the energy relative to the second-moment eigenvector transformation.

As an alternative to the ME form for the DOS, we tried functions of the type

$$n(\epsilon) = \left[\left| \sum_j^{n_{\max}} \lambda_j \epsilon_j \right|^k + \delta \right]^{-1},$$

where δ is a small number that prevents the denominator from going to zero, and the $\{\lambda_j\}$ values are determined from a NR search for the correct moments, as in ME. (For $k=2$, this form is essentially the “all-poles” model.⁵¹) Qualitatively, this form of DOS looks like the ME form, but is more peaked, especially as k is increased. Investigation of $k=1, 2$, and 4 within the charge-neutral atom-trace approximation yielded only small improvements in ΔE_{vac} for $n_{\max}=4$, raising it by 0.24, 0.13, and

0.06 eV, respectively. For $n_{\max}=6$, this approach was used to calculate the first-NN approximation, $\Delta E_{\text{vac}}^{(1)}$, with the result being a *decrease* in $\Delta E_{\text{vac}}^{(1)}$ for each of the three k values.

We also tried various “basis-set” approaches, in which the DOS was expressed as a linear combination of DOS’s predetermined from a variety of environments. This has some appealing features. Computing the DOS in this way does not require a nonlinear search. Also, the basis set DOS’s can be determined using more moments than the n_{\max} used in the final run; even the exact-TB DOS can be employed. Although more expensive, these calculations need be done only once. The resulting DOS thus has much more structure (and hopefully more accuracy) than if it is determined from the n_{\max} moments alone. Because the basis is not necessarily complete (there may not be a linear combination that exactly reproduces the desired moments), a polynomial correction can be added to the DOS to obtain the exact moments if desired. Although this type of approach looked promising initially, ultimately we could not find a viable method. We conclude that the low-order moments do not make a good measure set for distinguishing different environments. For example, consider the moments for $n_{\max}=6$ $\{\mu_0, \mu_1, \dots, \mu_6\}$ as a seven-dimensional vector. For an atom in the bulk crystal with lattice constant scaled by 1.025 (isotropically expanded by 2.5%) the resulting moment vector has a larger overlap with the vector for an atom adjacent to a vacancy (measured as the cosine between the two vectors) than it does with either the perfect bulk crystal or the bulk crystal expanded by 5%. As a result, the predicted energy has significant error.

Finally, in a different vein, we note that attempts to reparametrize the TB Hamiltonian to raise ΔE_{vac} were also unsuccessful. Perhaps ironically, the exact-TB vacancy formation energy in this model for Si (~ 6 eV) is very close to the cohesive energy (~ 6 eV), similar to the prediction that would result from a simple pair potential ($E_{\text{coh}} = \Delta E_{\text{vac}}$). In a search of the parameter space of $h(r)$ using a traced fourth-moment ME energy, only this trivial, unsatisfactory result [$h(r) \rightarrow 0$, leaving only the pairwise contribution] was found to offer significant improvement in ΔE_{vac} .

V. CONCLUSIONS

A general interatomic potential form can be constructed using low-order moments of the tight-binding Hamiltonian in conjunction with the maximum entropy approach to determine the density of states. The number of moments can be varied to trade accuracy for speed, and existing tight-binding parameter sets can be employed. Imposing atom-by-atom charge neutrality and tracing over rotationally invariant orbital subsets generally improves the quality. However, a careful study of the convergence of various properties as the number of moments is increased leads us to the conclusion that this approach may not be accurate enough for covalent materials. In particular, the vacancy formation energy for Si and C are predicted to be too low by more than 2 eV at ten mo-

ments. Attempts to improve the method were unsuccessful, leading us to speculate that this may be a general property of low-order moment methods. However, the approach may prove useful for metallic systems, in which the convergence is more rapid.

An important finding is that for environments in which all the atoms are equivalent, the calculated properties are often quite accurate (relative to exact TB), in spite of the deficiencies of the method. Properties that depend on truly defected environments offer a much more critical (and relevant) test of the potential.

ACKNOWLEDGMENTS

This work was performed under the auspices of the U.S. Department of Energy (DOE) through Los Alamos National Laboratory and was supported by the Office of Basic Energy Sciences, Division of Materials Sciences. The authors are grateful to R. Silver, I-H. Kwon, C. Z. Wang, K-M. Ho, A. Gibson, I. Morrison, J. Mercer, and A. P. Smith for helpful discussions, and to A. Gibson, I. Morrison, and R. Silver for communication of unpublished results.

-
- ¹J. K. Norskov and N. D. Lang, *Phys. Rev. B* **21**, 2131 (1980).
²M. J. Stott and E. Zaremba, *Phys. Rev. B* **22**, 1564 (1980).
³M. S. Daw and M. I. Baskes, *Phys. Rev. Lett.* **50**, 1285 (1983).
⁴M. W. Finnis and J. E. Sinclair, *Philos. Mag. A* **50**, 45 (1984); **53**, 161(E) (1986).
⁵X.-P. Li, R. W. Nunes, and D. Vanderbilt, *Phys. Rev. B* **47**, 10 891 (1993).
⁶M. S. Daw, *Phys. Rev. B* **47**, 10 895 (1993).
⁷G. Galli and M. Parrinello, *Phys. Rev. Lett.* **69**, 3547 (1992).
⁸F. Mauri, G. Galli, and R. Car, *Phys. Rev. B* **47**, 9973 (1993).
⁹W. Kohn, *Chem. Phys. Lett.* **208**, 167 (1993).
¹⁰E. B. Stechel, A. R. Williams, and P. J. Feibelman, *Phys. Rev. B* **49**, 10 088 (1994).
¹¹M. S. Daw and M. I. Baskes, *Phys. Rev. B* **29**, 6443 (1984).
¹²D. G. Pettifor, *Phys. Rev. Lett.* **63**, 2480 (1989).
¹³W. A. Harrison, *Phys. Rev. B* **41**, 6008 (1990).
¹⁴A. E. Carlsson, P. A. Fedders, and C. W. Myles, *Phys. Rev. B* **41**, 1247 (1990).
¹⁵A. E. Carlsson, *Phys. Rev. B* **44**, 6590 (1991).
¹⁶J. A. Moriarty and R. Phillips, *Phys. Rev. Lett.* **66**, 3036 (1991).
¹⁷S. M. Foiles, *Phys. Rev. B* **48**, 4287 (1993).
¹⁸D. G. Pettifor and M. Aoki, *Philos. Trans. R. Soc. London A* **334**, 439 (1991).
¹⁹P. Alinaghian, P. Gumbsch, A. J. Skinner, and D. G. Pettifor, *J. Phys. Condens. Matter* **5**, 5795 (1993).
²⁰R. Haydock, V. Heine, and M. J. Kelly, *J. Phys. C* **5**, 2845 (1972).
²¹R. Haydock, V. Heine, and M. J. Kelly, *J. Phys. C* **8**, 2591 (1975); see also the entire volume of *Solid State Phys.* **35**, (1980).
²²A. Gibson, R. Haydock, and J. P. LaFemina, *Phys. Rev. B* **47**, 9229 (1993).
²³S. Glanville, A. T. Paxton, and M. W. Finnis, *J. Phys. F* **18**, 693 (1988).
²⁴A. T. Paxton, A. P. Sutton, and C. M. M. Nex, *J. Phys. C* **20**, L263 (1987).
²⁵A. T. Paxton, *Philos. Mag. B* **58**, 603 (1988).
²⁶R. H. Brown and A. E. Carlsson, *Phys. Rev. B* **32**, 6125 (1985).
²⁷D. A. Drabold and O. F. Sankey, *Phys. Rev. Lett.* **70**, 3631 (1993).
²⁸A. P. Sutton, M. W. Finnis, D. G. Pettifor, and Y. Ohta, *J. Phys. C* **21**, 35 (1988).
²⁹J. Harris, *Phys. Rev. B* **31**, 1770 (1985).
³⁰W. M. C. Foulkes, Ph.D. thesis, University of Cambridge, 1987.
³¹F. Cyrot-Lackmann, *J. Phys. Chem. Solids* **29**, 1235 (1968).
³²J. C. Slater and G. F. Koster, *Phys. Rev.* **94**, 1498 (1954).
³³O. F. Sankey and D. J. Niklewski, *Phys. Rev. B* **40**, 3979 (1989).
³⁴J. D. Kress and A. F. Voter, *Phys. Rev. B* **43**, 12 607 (1991).
³⁵G. J. Ackland, M. W. Finnis, and V. Vitek, *J. Phys. F* **18**, L153 (1988).
³⁶E. T. Jaynes, *Papers on Probability, Statistics, and Statistical Physics* (Kluwer, Dordrecht, Holland, 1983).
³⁷L. R. Mead and N. Papanicalaou, *J. Math. Phys.* **25**, 2404 (1984).
³⁸I. Turek, *J. Phys. C* **21**, 3251 (1988).
³⁹G. L. Bretthorst (unpublished).
⁴⁰L. Goodwin, A. J. Skinner, and D. G. Pettifor, *Europhys. Lett.* **9**, 701 (1989).
⁴¹C. Z. Wang, C. T. Chan, and K. M. Ho, *Phys. Rev. B* **42**, 11 276 (1990).
⁴²R. N. Silver (private communication).
⁴³A. F. Voter, J. D. Kress, and R. N. Silver (to be published).
⁴⁴I. Morrison (private communication of results using method in Ref. 19).
⁴⁵A. Gibson (private communication of results using method in Ref. 22).
⁴⁶R. N. Silver, H. Röder, A. F. Voter, and J. D. Kress, in *Simulation MultiConference '95 Proceedings, High Performance Computing*, edited by A. Tentner (Society For Computer Simulation, San Diego, 1995), p. 200.
⁴⁷A. J. Skinner and D. G. Pettifor, *J. Phys. Condens. Matter* **3**, 2029 (1991).
⁴⁸W. A. Harrison, *Electronic Structure and the Properties of Solids* (Freeman, San Francisco, 1980).
⁴⁹O. K. Andersen, *Phys. Rev. B* **12**, 3060 (1975).
⁵⁰W. Xu and J. B. Adams, *Surf. Sci.* **301**, 371 (1994).
⁵¹W. H. Press, B. P. Flannery, S. A. Teukolsky, and W. T. Vetterling, *Numerical Recipes* (Cambridge University Press, Cambridge, 1989).